Paths towards synchronization: analytical treatment of completely connected networks

A España, Xavier Leoncini, E Ugalde

Combinatorics of the paths towards synchronization

A. España[a,b], X. Leoncini[a], E. Ugalde[b]

[a] *Aix Marseille Univ, Université de Toulon, CNRS, CPT, Marseille, France.*
[b] *Instituto de Física, Universidad Autónoma de San Luis Potosí, México.*

Abstract

In this paper, we introduce a codification of the paths towards synchronization for synchronizing flows defined over a network, as a way to characterize different possible synchronization sequences, and count them. The collection of paths toward synchronization defines a combinatorial structure: the transition diagram. We focus on the Laplacian flow over the completely connected graph and describe the corresponding transition diagram. This description applies as well to the Kuramoto flow over the same network, when considering initial conditions close to the synchronization manifold after a finite transient. We present as well some results concerning the Laplacian and Kuramoto flows over the complete bipartite graph.

1. Introduction

Synchronization phenomena are a long standing subject dating back at least to the observations of Huygens see for instance [1]. This field of research when considering coupled dynamical systems on networks has been very active since Kuramoto's seminal paper [2]. The first studies considered homogeneously coupled systems like global coupling, completely random coupling or coupling according to a regular network. A very complete account of those early work can be found in [3].

An approach to study the ways in which the components of an interacting system synchronize, depending on the interaction's topology, leads to the definition of synchronized subnetworks. As noticed in [4], the progression in connectivity

of the synchronized subnetwork as times increases qualitatively follows the dictates of the linearized dynamics. Given this remark it appears as natural that as a starting point in understanding paths towards synchronization, we should first try to understand this phenomenon in the context of the linear dynamical system defined by linear coupling among the components, that resumes to the Laplacian matrix on the considered network, for instance with global coupling. Under this flow, the coordinates of each initial condition converge to a common value, the so-called *consensus* [5]. This consensus is in fact the point in the synchronization manifold, attracting that particular initial condition, and the whole phenomenon can be regarded as a *full synchronization*. Furthermore, as will be shown, the paths towards full synchronization can be explicitly determined in this linear case. On the opposite, the nonlinear dynamics is not always necessarily fully synchronizing and noticeable differences between the nonlinear and the linearized flow appear as we increase the number of components, i.e size of the system. In contrast to the linearized flow, which is always landing on an attractor (i.e fully synchronizing), the synchronization when nonlinear couplings are considered, is subject to several conditions regarding the size of the network and its spectral dimension [6], among others.

So as a starting point of a study of paths towards synchronization, we consider a system for which full synchronization is insured. The asymptotic behavior is then trivial, but this gives us the opportunity to tackle the diversity of distinguishable paths towards synchronization, i.e tackle the transient dynamics and see how possibly the interaction's topology could affect these transient dynamics. Moreover, we can envision that to each distinguishable path towards synchronization we can associate an ensemble of initial conditions all taking the same path; this provides a way to partition the basin of attraction corresponding to the full synchronization, using distinguishable observable paths, and as such use time to uncover the complexity of the phenomenon and possibly encode information. For instance, once established we may be able to characterize the complexity of the system by counting the number of paths towards synchronization. Note that characterizing the complexity of the system by measuring the

diversity of paths is a classic topic that has been studied and illustrated, among others, in [7, 8, 9].

So the aim of this paper is to introduce the notion of synchronization sequences as a description of a path towards synchronization, and lay the ground for further possible studies. In fact this notion can be related to the connectivity matrix defined in [10]. In the case of a fully synchronizing system, the set of all the synchronizing sequences forms a transition diagram that encodes the whole transient dynamics towards synchronization. So after introducing some definitions, in this paper we settled as a starting point to study in full details this combinatorial structure in the case of the Laplacian dynamics on the fully connected network, and in some details in the case of the complete bipartite network. We characterize the transient dynamics on those networks by means of some topological features of the corresponding transition diagrams. We also analyze the applicability of this approach to the corresponding Kuramoto model.

The rest of the paper is organized as follows. After establishing the notations and the basic definitions in Section 2, we study in Section 3 the transition diagram of synchronization paths for the complete graph K_N. In Section 4 we study the applicability of the combinatorial description proper to the linear dynamics, to the corresponding Kuramoto model. Then, in Section 5 we present some results concerning the structure of the transition diagram for the complete bipartite graph $K_{N,N}$. Finally, in Section 6 we close the paper with some final remarks and comments.

2. Set-up

We will refer indistinctly by graph or network to an undirected graph $G = (V, E)$, with vertices in V and edges or links in E. On the contrary, a directed graph is a couple $D = (V, A)$ of vertices in V and arrows in A. An edge is a two-vertex set, its end vertices, while an arrow is an ordered pair of vertices. A subgraph of G is a graph $G' = (V', E')$ such that $V' \subset V$ and all the edges

in $E' \subset E$ have end vertices in V'. A path in G is a sequence of vertices such that each couple of consecutive vertices form an edge, while a path in D is an ordered sequence of vertices $v_1 \to v_2 \to \cdots \to v_n$ such that each couple of consecutive vertices forms an arrows. In this last case we say that v_1 is the starting vertex of the path and v_n the ending one, besides $n-1$, the number of arrows in the sequence, is the length of the path. A graph is connected if each couple of vertices belongs to a path. Any graph can be decomposed in a unique way as a disjoint union of connected subgraphs, called connected components.

We fix a graph $G = (V, E)$ and consider a system of coupled differential equations on I^V, where I is either $\mathbb{R}$ or the circle S^1. The flow is generated by a system of ODEs coupled according to the edges in E which represent the interactions between the particles.

We will focus on the Laplacian flow on G, which is the linear system defined by

$$\frac{dx_v}{dt} = (L\,x)_v = \sum_{u \in V : \{u,v\} \in E} (x_u - x_v), \text{ with } x_v \in \mathbb{R} \text{ for each } v \in V. \tag{1}$$

Here L is the Laplacian matrix of G, given by $L(v, v') = \sum_{u \in V : \{u,v\} \in E} (\mathbb{1}_{\{u\}} - \mathbb{1}_{\{v\}})(v')$. The synchronizing dynamics of the Laplacian flow is preserved in part by the Kuramoto flow defined in $(S^1)^V$ by the system of ODEs

$$\frac{dx_v}{dt} = \sigma \sum_{u \in V : \{u,v\} \in E} \sin(x_u - x_v), \tag{2}$$

where $\sigma \in \mathbb{R}^+$ is the strength of the coupling. In both flows, the diagonal, also known as *synchronization manifold*:

$$\mathcal{D} = \{x \in I^V : x_u = x_v \ \forall \ u, v \in V\}, \tag{3}$$

is an attractor, i.e., it is such that $\lim_{t \to \infty} \operatorname{dist}(x(t), \mathcal{D}) = 0$, for each initial condition in a neighborhood of $\mathcal{D}$. Indeed, it is a global attractor for the Laplacian flow and, since the linearization of the Kuramoto flow around the diagonal is proportional to the Laplacian flow, applying a Hartman-Grobman argument we conclude that it follows a similar converging dynamics in a small neighborhood of the diagonal.

In order to measure the degree of synchronization at a given time, we fix a precision $\epsilon > 0$ and declare that two neighboring sites are ϵ-synchronized if their distance does not exceed ϵ. Seeing as active each connection between neighboring sites which are ϵ-close, we define a subnetworks containing all the active connections. The determination and evolution of this subnetwork is the main objective of the present work. Hence, to each fixed threshold $\epsilon > 0$ and every configuration $x \in \mathbb{R}^V$, we associate an ϵ-synchronized subnetwork $G_x = (V, E_x)$, where $E_x \subset E$ is the collection of edges

$$E_x = \{\{u, v\} \in E : |x_u - x_v| \leqslant \epsilon\}. \tag{4}$$

For the systems under consideration, $G_{x(t)} \to G$ as $t \to \infty$ provided the initial condition is sufficiently close to the diagonal. Since there is a finite number of subnetworks, then for each suitable initial condition $x \in \mathbb{R}^V$ there exists a finite sequence of switching times $t_0 = 0 < t_1 < t_2 < \cdots < t_\ell$ and a corresponding sequence of ϵ-synchronized subnetworks $(G_x, G_{x(t_1)}, \ldots, G_{x(t_\ell)})$ such that $G_{x(t_\tau)} \neq G_{x(t_{\tau+1})}$, for each $0 \leqslant \tau < N$, and $G_{x(t)} = G_{x(t_\tau)}$ with $\tau = \max\{0 \leqslant j \leqslant \ell : t \geqslant t_j\}$. These sequence of subnetworks of G codify the progression of transient synchronizing patterns. By taking ϵ sufficiently small, all the possible synchronizing sequences can be obtained by varying the initial condition x inside the basin of attraction of the diagonal. As a sidenote, we may notice that the synchronizing sequence can be seen as time evolving network as more and more ϵ-synchronized neighbours are appearing, and as such the sequence can be seen as a deterministic example of a temporal network [11].

In the case of highly symmetric networks, instead of the ϵ-synchronized subnetworks it is convenient to use another combinatorial structure that at the same time encodes the subnetwork and respects some of the symmetries which are preserved by the dynamics. As we will see below, this eases the description of the evolution of the synchronized subnetworks. Hence, the whole synchronizing dynamics on G can be compiled in a single combinatorial superstructure. This superstructure is a transition diagram whose vertices are in correspondence (not necessarily injective) with ϵ-synchronized subnetworks in such a way

that the collection of all the paths in the transition diagram is equivalent to the set of all the observable sequences of ϵ-synchronized subnetworks. To study this dynamics, it is enough to see the diagram with other labels that allows to encode the G_x. To be more precise, the transition diagram is a directed graph $\mathcal{T}_\epsilon = (V_\epsilon, A_\epsilon)$ whose vertices, V_ϵ are combinatorial objects containing all the information we need to determine the ϵ-synchronized subnetworks and the arrows, A_ϵ, are transitions between those structures which are consistent with the evolution of the synchronized subnetworks. The correspondence between objects in V_ϵ and ϵ-synchronized subnetworks is achieved via a mapping

$$\lambda : V_\epsilon \to \mathcal{E}_\epsilon, \tag{5}$$

that labels each vertex in the transition diagram with an ϵ-synchronized subnetwork. The labelling λ is such that $(G_0, G_1, \ldots, G_\ell)$ is a realizable sequence of ϵ-synchronized subnetworks if and only if there exists a path $v_0 \to v_1 \to \cdots \to v_\ell$ in $\mathcal{T}_\epsilon$ such that $G_n = \lambda(v_n)$ for $0 \leqslant n \leqslant \ell$, we will see these encodings in detail later.

In general, the set $\mathcal{E}_\epsilon$ of all the ϵ-synchronized subnetworks changes with ϵ. Nevertheless, for ϵ sufficiently small, the set of ϵ-synchronized subgraphs defined by initial conditions in a small neighborhood of $\mathcal{D}$ becomes independent of ϵ. For the Laplacian flow, the set $\mathcal{E}_\epsilon$ of all possible synchronized subnetworks is independent of ϵ as long as $\epsilon > 0$. Even if $\mathcal{E}_\epsilon$ is independent of ϵ, the corresponding transition diagram may change with ϵ. This, nevertheless, does not happen in the linear case, since for each initial condition $x \in \mathbb{R}^V$, the corresponding sequence $(G_x, G_{x(t_1)}, \ldots, G_{x(t_\ell)})$ of ϵ-synchronized subnetworks coincides with the sequence $(G_y, G_{y(t_1)}, \ldots, G_{y(t_\ell)})$ of ϵ'-synchronized subnetworks determined by $y = x\,\epsilon'/\epsilon$. Indeed, by Equation (4) and by the linearity of the system, $\{u, v\} \in E_x$ is equivalent to $|x_u - x_v| \leqslant \epsilon$, hence $|x_u - x_v| = \epsilon/\epsilon'|y_u - y_v| \leqslant \epsilon$, therefore $|y_u - y_v| \leqslant \epsilon'$, which is equivalent to $\{u, v\} \in E_y$. From this it follows that the collection of ϵ-synchronized sequences does not depend on ϵ in the linear case. Clearly, since this number is finite, each synchronized sequence can be

realized by an infinite number of initial conditions, which in principle allows to realize some partition of the initial phase space, i.e., the basin of attraction of the final synchronized state.

We will restrict our study to the following families of networks:

A. The complete graph K_N, for which $V = \{1, 2, \ldots, N\}$ and $E = \{\{u, v\} : 1 \leqslant u < v \leqslant N\}$.

B. The complete bipartite graph $K_{N,N}$, where $V = \{1, 2, \ldots, 2N\}$ and $E = \{\{u, N + v\} : 1 \leqslant u, v \leqslant N\}$.

Considering these families, we address the following questions:

1. Given the underlying network, which subgraphs are realizable as synchronizing subnetworks? How large is this collection and how does it grow with the size of the underlying graph?
2. Given an underlying network, what is the structure of the transition diagram? In particular, what is the longest path and what is the resulting distribution of path lengths?

3. The transition diagram for K_N

The Laplacian matrix for K_N diagonalizes in the basis $\{u^1, u^2, \ldots, u^N\}$, where $u^1 := \sum_{n=1}^{N} \mathsf{e}^n$ and, for each $n \geqslant 1$, $u^n := \mathsf{e}^n - \mathsf{e}^1$, where e^n denotes the n-th vector of the canonical basis. Indeed, $Lu^1 = 0$ and $Lu^n = -N\,u^n$ for each $n \geqslant 2$. Consider now an initial condition $x \in \mathbb{R}^N$. Such an initial condition can be decomposed as $x = \bar{x}\,u^1 + \sum_{n=1}^{N-1}(x_{n+1} - \bar{x})\,u^n$, where $\bar{x} := \left(\sum_{n=1}^{N} x_n(0)\right)/N$. Therefore

$$x(t) = \bar{x}\,u^1 + e^{-N\,t} \sum_{n=1}^{N-1} (x_{n+1} - \bar{x})\,u^n = \sum_{n=1}^{N} \left(\bar{x}\left(1 - e^{-N\,t}\right) + e^{-N\,t} x_n\right) \mathsf{e}^n,$$

for all $t \in \mathbb{R}$. From this, it follows that

$$x_n(t) - x_m(t) = e^{-N\,t}(x_n - x_m), \tag{6}$$

for all $t \in \mathbb{R}$ and each $1 \leqslant m, n \leqslant N$. Hence, the edge $\{n, m\}$ belongs to the ϵ-synchronized subnetwork $G_{x(t)}$, for all times exceeding $t_{n,m} = (\log|x_n - x_m| - \log(\epsilon))/N$.

Without loss of generality we may assume that $x_1(0) \leqslant x_2(0) \leqslant \cdots \leqslant x_N(0)$ which, by Equation (6), ensures that $x_1(t) \leqslant x_2(t) \leqslant \cdots \leqslant x_N(t)$ for all t.

In order to take advantage of the fact that the Laplacian flow preserves the order of the coordinates, we will define the transition diagram not over the synchronized subnetworks but over another combinatorial object that encodes both the synchronized subnetworks, and recognizes the order of the coordinates. By doing so we will facilitate the description of the transition diagrams since the coding we use allows us to easily determine the order of apparition of new edges in the synchronized sequence. This coding is not only convenient but necessary if one wants to keep track of the order of the coordinates. We codify ϵ-synchronized subnetwork G_x, determined by the ordered configuration $x_1 \leqslant x_2 \leqslant \cdots \leqslant x_N$ by the increasing function $\phi_x : \{1, 2, \ldots, N\} \to \{1, 2, \ldots, N\}$ given by

$$\phi_x(m) = \max\{n \geqslant m : \, x_n \leqslant x_m + \epsilon\}. \tag{7}$$

Clearly ϕ_x is increasing and such that $\phi_x(n) \geqslant n$ for each $1 \leqslant n \leqslant N$, i.e., $\phi_x \geqslant \mathrm{Id}$. Here and below Id denotes the identity function in $\{1, 2, \ldots, N\}$. We present an example of the construction of the increasing function from a given initial condition, in Figure 1.

By the arguments developed in the Appendix Appendix A, we know that the collection

$$\Phi_N := \{\phi : \{1, \ldots, N\} \to \{1, \ldots, N\} \text{ increasing and such that } \phi \geqslant \mathrm{Id}\}, \tag{8}$$

is in a one-to-one correspondence with the collection of all ϵ-synchronized subnetworks of K_N defined by initial conditions satisfying $x_1 \leqslant x_2 \leqslant \cdots \leqslant x_N$. The correspondence is given by

$$\phi \mapsto (\{1, 2, \ldots, N\}, E_\phi) \text{ where } E_\phi = \{\{m, n\} : \, \min(m, n) \leqslant \phi(\max(n, m))\}. \tag{9}$$

In this case, the coding (5) which associates increasing functions to synchronized subnetworks is given by Equation (9).

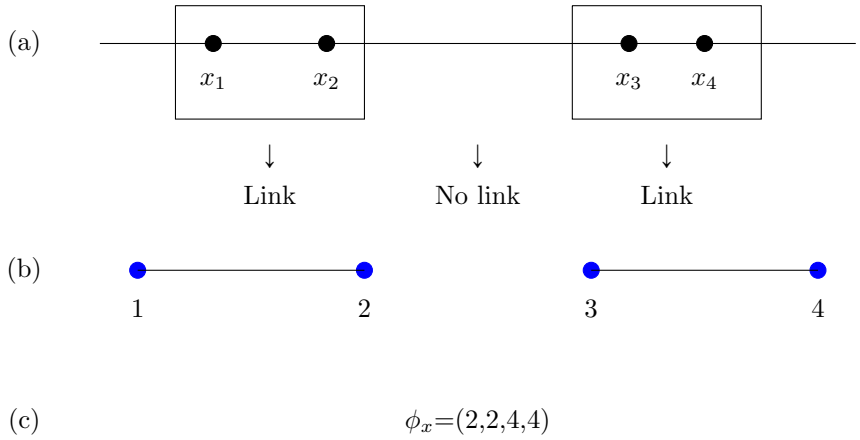

Figure 1: In (a), an example of the values of $x = (x_1, x_2, x_3, x_4)$ are illustrated with black dots. To construct G_x, according to Equation (4), it is enough to observe that x_1 and x_2 are inside one ϵ-neighborhood, and x_3 and x_4 in another, which implies that in (b) there are links between the vertices 1 and 2 as well as between vertices 3 and 4. In (c), the increasing function ϕ_x associated with x is depicted. The information in ϕ_x can be read as follows: The furthest vertex connected with vertex 1 is vertex 2, vertex 2 does not reach vertex 3, and vertex 3 reaches vertex 4, which is the last one.

150

The collection Φ_N is equivalent to a well-studied combinatorial set, the set $\mathcal{D}_{2N}$ of Dyck paths of length $2N$. This set is in turn equivalent to the set of valid $2N$-parenthesis configurations. All these combinatorial sets have a cardinality given by the Catalan numbers [12],

$$|\Phi_N| = C_N := \frac{1}{N+1}\binom{2\,N}{N}. \tag{10}$$

Taking into account the equivalence established in the previous paragraph, each sequence of ϵ-synchronized subnetworks $(G_x, G_{x(t_1)}, \ldots, G_{x(t_\ell)})$ generated by an ordered initial condition x, is faithfully codified by the corresponding sequences

of increasing functions $(\phi_x, \phi_{x(t_1)}, \ldots, \phi_{x(t_\ell)})$ in Φ_N defined by Equation (7). Clearly the function $t \mapsto \phi_{x(t)}(n)$ increases with t for each n fixed, and converges to $\phi_{x(t)} = N$ at the time $t_{1,N} = (\log(x_N - x_1) - \log(\epsilon))/N$. Due to the monotonicity, the length ℓ of an ϵ-synchronized sequences is upper bounded by the number of edges in K_N, i.e., $\ell \leqslant N(N-1)/2$. As mentioned above, the switching times $t_1 < t_2 < \cdots < t_\ell$ are completely determined by the increments $x_n - x_m$, with $m < n$. Let us assume that all those increments are different from zero and pairwise different. We will say that a path satisfying this condition is typical. Clearly, the non-typical paths correspond to initial conditions in a set of zero Lebesgue measure in $\mathbb{R}^N$. Hence, for typical paths, two consecutive functions in the sequence $(\phi_0, \phi_1, \ldots, \phi_\ell) := (\phi_x, \phi_{x(t_1)}, \ldots, \phi_{x(t_\ell)})$ differ at a single point. Let us denote by $\delta_n \in \{0,1\}$ the characteristic function of the singleton $\{n\}$. Hence $\phi_{\tau+1} = \phi_\tau + \delta_{n_\tau}$ for some $n_\tau \in \{1, 2, \ldots, N\}$ satisfying the condition $\phi_\tau(n_\tau) < \phi_\tau(n_\tau + 1)$. Hence an admissible sequence $(\phi_0, \phi_1, \ldots, \phi_\ell)$ can be obtained by choosing a valid initial function $\phi_0 \in \Phi_N$, then for each $\tau \geqslant 0$, a point $n_\tau \in \{1, 2, \ldots, N-1\}$ such that $\phi_\tau(n_\tau) < \phi_\tau(n_\tau + 1)$ to update $\phi_{\tau+1} = \phi_\tau + \delta_{n_\tau}$. Nevertheless, not all the sequences obtained in this way are realizable as synchronizing sequences. The sequence $(n_\tau)_{0 \leqslant \tau < \ell}$ of jump sites is determined by an order in the increments $\Delta := \{\Delta_{n,k} := x_{n+k} - x_n : 1 \leqslant n < n + k \leqslant N\}$ in such a way that the τ-th smallest increment in Δ is of the kind $\Delta_{n_\tau,k}$. Hence, to each valid strict ordering in Δ corresponds a unique realizable path towards synchronization.

One can easily verify that not all the admissible paths are realizable. The simplest counterexample happens for $N = 4$ (for $N = 2, 3$ all admissible sequences are realizable). In this case the sequence $\mathrm{Id} \mapsto (2,2,3,4) \mapsto (2,2,4,4) \mapsto (2,3,4,4) \mapsto (2,4,4,4) \mapsto (3,4,4,4) \mapsto (4,4,4,4)$, which corresponds to the sequences of jump sites $(1,3,2,2,1,1)$, is not realizable since the first two transitions indicate that $x_2 - x_1 < x_4 - x_3$ but transitions four and five imply that $x_4 - x_2 < x_3 - x_1$, which is contradictory. The total number of admissible paths for $N = 4$ is sixteen. On the other hand, the total number of realizable paths

is ten, and the associated valid strict orderings are shown in Table 1.

$\Delta_{1,1} < \Delta_{2,1} < \Delta_{3,1} < \Delta_{1,2} < \Delta_{2,2} < \Delta_{1,3}$	$\Delta_{1,1} < \Delta_{2,1} < \Delta_{1,2} < \Delta_{3,1} < \Delta_{2,2} < \Delta_{1,3}$
$\Delta_{1,1} < \Delta_{3,1} < \Delta_{2,1} < \Delta_{1,2} < \Delta_{2,2} < \Delta_{1,3}$	$\Delta_{2,1} < \Delta_{1,1} < \Delta_{3,1} < \Delta_{1,2} < \Delta_{2,2} < \Delta_{1,3}$
$\Delta_{2,1} < \Delta_{1,1} < \Delta_{1,2} < \Delta_{3,1} < \Delta_{2,2} < \Delta_{1,3}$	$\Delta_{2,1} < \Delta_{3,1} < \Delta_{1,1} < \Delta_{2,2} < \Delta_{1,2} < \Delta_{1,3}$
$\Delta_{2,1} < \Delta_{3,1} < \Delta_{2,2} < \Delta_{1,1} < \Delta_{1,2} < \Delta_{1,3}$	$\Delta_{3,1} < \Delta_{1,1} < \Delta_{2,1} < \Delta_{2,2} < \Delta_{1,2} < \Delta_{1,3}$
$\Delta_{3,1} < \Delta_{2,1} < \Delta_{1,1} < \Delta_{2,2} < \Delta_{1,2} < \Delta_{1,3}$	$\Delta_{3,1} < \Delta_{2,1} < \Delta_{2,2} < \Delta_{1,1} < \Delta_{1,2} < \Delta_{1,3}$

Table 1: The ten different orderings of the increments for a typical initial conditions in $\mathbb{R}^4$.

Each ordering in Table 1 uniquely determines an observable path towards synchronization. The corresponding paths towards synchronization are organized in a transition diagram, depicted in Figure 2.

As mentioned above, the path towards synchronization for the initial condition x is given by the sequence $(G_x, G_{x(t_1)}, \ldots, G_{x(t_\ell)})$ of synchronizing subnetwork, which is equivalent to a sequences of increasing functions $(\phi_x, \phi_{x(t_1)}, \ldots, \phi_{x(t_\ell)})$ in Φ_N. The sequence $(\phi_x, \phi_{x(t_1)}, \ldots, \phi_{x(t_\ell)})$ is completely determined by the order of the increments Δ. Each ordering of increments determines the sequence $(n_\tau)_{0 \leqslant \tau < \ell}$ of sites where consecutive increasing functions differ, i.e., the sites n_τ such that $\phi_{x(t_{\tau+1})} - \phi_{x(t_\tau)} = \delta_{n_\tau}$ for each $0 \leqslant \tau < \ell$. Hence, each valid ordering in Δ corresponds to a unique realizable path towards synchronization. Therefore, the total number of paths toward synchronization is given by the number of different orderings Δ which can be obtained from an ordered vector $x \in \mathbb{R}^N$. This is a combinatorial problem which has been treated in the literature in the context of the so called Golomb rulers [13], that is, the problem of counting the number of valid orders is equivalent to counting the combinatorially distinct Golomb rulers. Below we will explain how this equivalence is established.

A Golomb ruler with N marks is a vector $a \in \mathbb{Z}^N$ with $a_1 < a_2 < \cdots < a_N$, such that no two increments $a_{n+k} - a_n$, where $1 \leqslant n < N$, and $1 \leqslant k \leqslant N - n$

coincide. Hence, a Golomb ruler is nothing but a typical initial condition with integer entries.

To each typical initial condition $x \in \mathbb{R}^N$ we may associate a Golomb ruler as follows. Since x is typical, then both $\epsilon_1 = \min\{\Delta_{n,k} : 1 \leqslant n < N, 1 \leqslant k < N-n\}$ and $\epsilon_2 = \min\{|\Delta_{n,k} - \Delta_{m,\ell}| : (m,k) \neq (n,\ell) : 1 \leqslant n < N, 1 \leqslant k < N-n, 1 \leqslant m < N, 1 \leqslant \ell < N-m\}$ are strictly positive. Let $p \in \mathbb{N}$ be such that $p \cdot \min(\epsilon_1, \epsilon_2/4) > 1$, and for each $1 \leqslant n \leqslant N$ let $q_n := \max\{q \in \mathbb{Z} : q/p \leqslant x_n\}$. The vector $q = (q_1, q_2, \ldots, q_N) \in \mathbb{Z}^N$ is the desired Golomb ruler. Indeed, since $p\,\epsilon_1 > 1$, then for each $1 \leqslant n < N$ we have

$$q_n \leqslant p\,x_n \leqslant p\,(x_{n+1} - \epsilon_1) \leqslant q_{n+1} + 1 - p\,\epsilon_1 < q_{n+1}.$$

On the other hand, whenever $\Delta_{n,k} > \Delta_{m,\ell}$ we have

$$(q_{n+k} - q_n) - (q_{m+\ell} - q_m) \geqslant p(\Delta_{n,k} - \Delta_{m,\ell} - 4/p) > p(\epsilon_2 - 4/p) > 0.$$

Two Golomb rulers are combinatorially equivalent if they determine the same ordering in their differences, i.e., $a, b \in \mathbb{R}^N$ are equivalent if and only if $((a_{n+k} - a_n) - (a_{m+\ell} - a_m))((b_{n+k} - b_n) - (b_{m+\ell} - b_m)) > 0$ for each $1 \leqslant m, n < N$ and $1 \leqslant k < n$, $1 \leqslant \ell < m$. Hence, the number Golomb(N) of classes of Golomb rulers with N marks, gives the number of paths towards synchronization, i.e.,

$$\text{Number of paths towards synchronization for } K_N = \text{Golomb}(N). \tag{11}$$

The growth of this quantity with the dimension N, is a measure of complexity similar to the topological complexity of discrete-time dynamical systems. In the case of a discrete-time dynamical system, the topological complexity counts the growth of the number of distinguishable trajectories as a function of time. In our case, Golomb(N) counts the number of distinguishable paths towards synchronization, not as a function of time, but of the dimension of the system.

A Golomb ruler $a \in \mathbb{Z}$ is also characterized by the fact that all the sums $a_m + a_n$ are different. Indeed, since

$$\text{sign}((a_{n+k} - a_n) - (a_{m+\ell} - a_m)) = \text{sign}((a_{n+k} + a_m) - (a_{m+\ell} + a_n)),$$

the number of combinatorially different Golomb rules is given by the number of different orderings for $S = \{a_m + a_n : 1 \leqslant m < n \leqslant N\}$ which is equal to the number of different orderings for $P = \{a_m\, a_n : 1 \leqslant m < n \leqslant N\}$. This number is relevant in problem of quantum entanglement [14]. The sequence Golomb(N) appears in the On-line Encyclopedia of Integer Sequences under the entry A237749 [15], where the first nine terms, which we present in Table 2, are explicitly computed.

N	Golomb(N)
1	1
2	1
3	2
4	10
5	114
6	2608
7	107498
8	7325650
9	771505180

Table 2: Number of classes of Golomb rulers.

The computation of Golomb(N) remains an open problem. Easy bounds for this number are shown in Equation (12). The lower bound can be obtained by counting all the orderings of the first differences $x_{i+1} - x_i$ for $1 \leqslant i \leqslant N-1$, while the upper bound results taking all the ordering of all the differences $x_i - x_k$ for $1 \leqslant k < i \leqslant N$. Form this we obtain,

$$(N-1)! < \text{Golomb}(N) < \binom{N}{2}!. \tag{12}$$

An exact non-trivial upper bound, based on a result by M. R. Thrall [16], was found by N. Johnston [17]. It establishes that

$$\text{Golomb}(N) \leqslant \frac{\prod_{n=1}^{N-1} n!}{\prod_{n=1}^{N}(2n-1)!}\ \left(\frac{N(N+1)}{2}\right)! \tag{13}$$

which furnishes an upper bound for the number of paths towards synchronization as well.

We do not intend to make an exhaustive characterization of the transition diagram, but from the concepts already defined, certain characteristics can be calculated, such as: the number of synchronized sequences of length ℓ, the distribution of lengths of the path towards synchronization. From this we compute the mean length and the most frequent length of paths. Furthermore, we can extrapolate the behavior of these quantities for increasingly large dimensions.

The transition diagram for K_N has a hierarchical structure with the disconnected subnetwork, codified by the identity function $\mathrm{Id} \in \Phi_N$, at the top, and the completely connected network, codified by the constant function $\mathbf{N}(n) = N$, at the bottom. Since we are considering only typical initial conditions, at each transition only one new edge appears in the ϵ-synchronized subnetwork. At level ℓ, from top to bottom, we place all the subnetworks which can be reached from the disconnected subnetwork after exactly ℓ transition. These subnetworks are precisely those having exactly ℓ edges, and are therefore codified by increasing functions $\phi \in \Phi_N$ such that $\sum_{n=1}^{N}(\phi(n) - n) = \ell$. In particular, the maximal length of a synchronizing sequences is $l_{\max} = \sum_{n=1}^{N}(N-n) = N(N-1)/2$. From our discussion above it readily follows that the number $F_N(\ell)$ of synchronized sequences of length ℓ is given by number of Dyck paths of length $2N$ and area $N^2 - \ell$, i.e.,

$$F_N(\ell) := \left| \left\{ \phi \in \Phi_N : \sum_{n=1}^{N} \phi(n) = N^2 - \ell \right\} \right|. \tag{14}$$

These quantities can be computed from the generating polynomials

$$P_N(t) := \sum_{\phi \in \Phi_N} t^{\mathrm{area}(\phi)} = \sum_{\ell=0}^{\frac{N(N-1)}{2}} F_N(\ell)\, t^{\frac{N(N-1)}{2} - \ell},$$

where $\mathrm{area}(\phi) := \sum_{n=1}^{N}(\phi(n) - n)$ denotes the area under the Dyck path determined by the increasing function ϕ. The generating polynomials can be

determined by using the recurrence relation

$$P_N(t) = \sum_{n=0}^{N-1} t^n \, P_n(t) \, P_{N-n-1}(t) \tag{15}$$

with initial conditions $P_0 = 0$, derived by Carlitz and Riordan [18] (see [19] as well). Although there is no closed form for $F_N(\ell)$, the recurrence relation above allows to directly compute these distributions and to establish its asymptotic behavior. In Table 3 we show $F_N(\ell)$ for $2 \leqslant N \leqslant 8$.

N	$F_N(\ell)$
2	(1,1)
3	(1,1,2,1)
4	(1,1,2,3,3,3,1)
5	(1,1,2,3,5,5,7,7,6,4,1)
6	(1,1,2,3,5,7,9,11,14,16,16,17, 14,10,5,1)
7	(1,1,2,3,5,7,11,13,18,22,28,32,37,40,44,43,40,35,25,15,6,1)
8	(1,1,2,3,5,7,11,15,20,26,34,42,53,63,73,85,96,106,113,118,118,115,102,86,65,41,21,7,1)

Table 3: Number $F_N(\ell)$ of functions $\phi \in \Phi_N$ codifying a subnetworks starting a synchronizing path of length ℓ.

The normalized cumulative distribution, $f_N : [0,1] \to [0,1]$, is defined by

$$f_N(x) = \frac{1}{C_N} \sum_{n \leqslant x \times N(N-1)/2} F_N(x), \tag{16}$$

where F_N is given by Equation (14) and C_N the N-th Catalan number. By using the recurrence shown in Equation (15), we numerically computed $f_N(x)$ for increasing values of N, and observe that f_N approaches an absolutely continuous limit distribution $x \mapsto f(x)$ whose density $\rho(x) := d\,f(x)/dx$ is closely approached by the curve depicted in Figure 3. Hence, for N sufficiently large and $\delta > 0$ sufficiently small, the proportion of paths of length $N(N-1)(x \pm \delta)/2$

is approximatively $\rho(x)\,\delta$. As shown in the figure, our numerical computation suggest that ρ is continuous, unimodal, and negatively skewed.

Summarizing, the transition diagram for K_N is composed by levels $\mathrm{L}_0, \mathrm{L}_1, \ldots, \mathrm{L}_{N(N-1)/2}$, in such a way that each path towards synchronization passes through levels of increasing index until reaching level $N(N-1)/2$ which contains only the complete graph, representing the full ϵ-synchronization. A typical initial condition starting at L_n, will take $N(N-1)/2 - n$ steps to attain the complete graph. The number of subnetworks at level $n = N(N-1)/2 - \ell$ is given by $F_N(\ell)$, defined by Equation (14). The number of subnetworks at each level increases monotonously from 1 to

$$\mathrm{mode}_N(\ell) := \max_{1 \leqslant \ell \leqslant N(N-1)/2} F_N(\ell) \approx 0.632\,\frac{N\,(N-1)}{2}, \tag{17}$$

and then decreases monotonously to 1 as depicted in Figure 3. Being the distribution of those lengths negatively skewed, the mean length of these paths is smaller than the most frequent length and we have

$$\langle \ell \rangle_N := \frac{\sum_{\ell=1}^{N(N-1)/2} \ell\, F_N(\ell)}{C_N} \approx 0.523\,\frac{N\,(N-1)}{2} < \mathrm{mode}_N(\ell).$$

From the calculations above, we can get an idea of some features of a typical synchronization path in the Laplacian of the complete graph, for example, if we were to take a random ordered initial condition of dimension N, then its associated synchronization path would most likely be of length as in Equation (17).

4. Applicability to the Kuramoto model

Although the above results concern the Laplacian flow, they apply as well to the Kuramoto model for initial conditions inside a neighborhood of the synchronization manifold. To be more precise, inside a neighborhood of the diagonal, the ϵ-synchronized subnetworks of the Kuramoto model can be encoded as increasing functions, exactly as in the linear case. Furthermore, for each initial

condition in this neighborhood, there is a time from which its path towards synchronization is described by the increasing sequences of increasing functions determined by the order of coordinate's increments, in exactly the same way as in the linear case. Indeed, what determines the applicability of the combinatorial scheme developed in the previous section is not the linear nature of the dynamics but the fact that the order of the coordinates, as well as the order of their increments, are both preserved by the dynamics. This order preservation takes place from a finite time for all initial conditions in a neighborhood around the synchronization manifold.

Let us now determine the neighborhood where the order of the coordinates is preserved by the flow. According to Equation (2) the dynamics of an coordinates' difference, $x_n - x_m$, is governed by the equation

$$\begin{aligned} \frac{d(x_n - x_m)}{dt} &= \sigma \left(\sum_{k=1}^{N} \sin(x_k - x_n) - \sin(x_k - x_m) \right), \\ &= \sigma\, R \left(\sin(\Theta - x_n) - \sin(\Theta - x_m) \right), \\ &= -2\,\sigma\, R\, \cos\left(\Theta - \frac{x_n + x_m}{2} \right) \sin\left(\frac{x_n - x_m}{2} \right), \end{aligned} \tag{18}$$

with $R \geqslant 0$ and $\Theta \in [-\pi, \pi]$ given by $R\, e^{i\Theta} = \left(\sum_{k=1}^{N} \cos(x_k) \right) + i \left(\sum_{k=1}^{N} \sin(x_k) \right)$. According to Equation (18), if x_n and x_m would merge at a given time τ, then we would have $d(x_n - x_m)/dt|_{t=\tau} = 0$ which would imply that $x_n = x_m$ for all $t \geqslant \tau$. This is impossible being $x_n - x_m$ a differentiable function, therefore no crossing of coordinates is possible at finite time, and therefore the cyclic order in the coordinates is preserved under the flow. Now, by taking $\max_{1 \leqslant n \leqslant N} |\Theta - x_n| \leqslant \pi/2$ we ensure that $\cos\left(\Theta - (x_n + x_m)/2\right) \geqslant 0$ and that the signs of $\sin\left((x_n - x_m)/2\right)$ and $x_n - x_m$ be the same. Hence, in this neighborhood $d(x_n - x_m)/dt$ and $x_n - x_m$ have opposite signs, which ensures that $|x_n - x_m|$ converged monotonously to zero while both x_n and x_m converge monotonously to Θ. This authorizes us to code the ϵ-synchronized subnetworks as increasing function, as we did in the Laplacian case.

By an innocuous change of variables we can make $\Theta = 0$ and, if necessary, relabel the coordinates to ensure that $x_1 < x_2 < \ldots < x_N$. Let us consider

two coordinate increments $\Delta_{n,k} := x_{n+k} - x_n$ and $\Delta_{m,\ell} := x_{m+\ell} - x_m$. The evolution of the difference between these increments is governed by the equation

$$\frac{d(\Delta_{n,k} - \Delta_{m,\ell})}{dt} = -2\,\sigma\,R\left\{\cos\left(\frac{s_{n,k}}{2}\right)\sin\left(\frac{\Delta_{n,k}}{2}\right) - \cos\left(\frac{s_{m,\ell}}{2}\right)\sin\left(\frac{\Delta_{m,\ell}}{2}\right)\right\},$$

with $s_{n,k} = x_n + x_{n+k}$ and similarly for $s_{m+\ell}$. Each time we have a crossing, $\Delta_{n,k} = \Delta_{m,\ell}$, the sense of the subsequent splitting is determined by the sign of $\cos(s_{m,\ell}/2) - \cos(s_{n,k}/2)$. Hence, in two consecutive crossings the sign of $\cos(s_{m,\ell}/2) - \cos(s_{n,k}/2)$ has to change. Without lost of generality we may assume that $x_n < x_m$. We have to consider all the possible arrangements for the other two coordinates x_{n+k}, $x_{m+\ell}$, and the position of the 4-tuple of coordinates with respect to the origin. Being the order of the coordinates preserved by the flow, we can already establish that $\Delta_{n,k} > \Delta_{m,\ell}$ for all $t \geqslant 0$, in the case $x_n < x_m < x_{m+\ell} < x_{n+k}$ at $t = 0$. Notice that for initial conditions in the neighborhood $\max_{1\leqslant n\leqslant N} |x_n| \leqslant \pi/2$, the signs of $\cos(s_{m,\ell}/2) - \cos(s_{n,k}/2)$ and $|s_{m,\ell}| - |s_{n,k}|$ are opposite. Depending on the initial order of the coordinates, one of the following possibilities may occur at the first crossing.

a) $\mathrm{sign}(s_{m,\ell}) = \mathrm{sign}(s_{n,k})$, in which case $|s_{m,\ell}| - |s_{n,k}| = x_m - x_n$ or $|s_{m,\ell}| - |s_{n,k}| = x_n - x_m$.

b) $\mathrm{sign}(s_{m,\ell}) = -\mathrm{sign}(s_{n,k})$, in which case $|s_{m,\ell}| - |s_{n,k}| = x_m + x_n$ or $|s_{m,\ell}| - |s_{n,k}| = -(x_n + x_m)$.

As we have seen, in the considered neighborhood of the synchronization manifold, the coordinates' difference $x_m - x_n$ does not changes its sign. Therefore in case a) there cannot be a second crossing. For the case b), it is enough to notice that

$$\frac{d(x_n + x_m)}{dt} = -2\,\sigma\,R\,\sin\left(\frac{x_n + x_m}{2}\right)\cos\left(\frac{x_n - x_m}{2}\right).$$

Following the same argument as for the difference $x_n - x_m$, we readily deduce that $x_n + x_m$ cannot change sign, there cannot be a second crossing in case b) either. Hence, after all possible crossings have occurred, the path towards synchronization will be the one determined by the order of the resulting increments Δ, exactly as prescribed by the linear case.

It is always possible to find an initial condition x with $\max_{1\leqslant n\leqslant N}|x_n-\Theta|<\delta$, and coordinates $x_n, x_{n+k}, x_m, x_{m+\ell}$ such that $\Delta_{n,k}-\Delta_{m,\ell}$ changes its sign. For this it is enough to take a configuration such that $\Delta_{n,k}=\Delta_{m,\ell}$ and $0<s_{n,k}<s_{m,k}$, so that $d(\Delta_{n,k}-\Delta_{m,\ell})/dt<0$, and then reverse the time to obtain an initial condition with $\Delta_{n,k}>\Delta_{m,\ell}$ which will necessarily produce a crossing in a finite time.

In summary, the initial conditions satisfying $\max_{1\leqslant n\leqslant N}|x_n-\Theta|<\pi/2$ define ϵ-synchronized subnetworks which can be encoded by increasing function in Φ_N, exactly as in the linear case. Furthermore, all these initial conditions will eventually follow a path in the transition diagram obtained for the linear case. This path will be the one prescribed by the order of the increments, just as in the linear case.

5. Some results concerning $K_{N,N}$

Let us recall that the Laplacian matrix of L corresponding to the network $K_{N,N}$ has the following entries

$$L(i,j) \;=\; \begin{cases} 1, & \text{if } N<i\leqslant 2N \text{ and } 0<j\leqslant N \text{ or } N<j\leqslant 2N \text{ and } 0<i\leqslant N,\\ -N, & \text{if } i=j,\ 1\leqslant i,j\leqslant 2N,\\ 0, & \text{otherwise.}\end{cases}$$

An eigenbasis can be computed in terms of the canonical basis and written as the set $\mathcal{B}=\{u^m, v^n, w^n:\ 1\leqslant m\leqslant 2,\ 1\leqslant n\leqslant N-1\}$, where $u^1=\sum_{k=1}^{2N}\mathsf{e}^k$, $u^2=\sum_{k=1}^{N}(\mathsf{e}^k-\mathsf{e}^{k+N})$ and for each $n\geqslant 1$, $v^n=\mathsf{e}^{n+1}-\mathsf{e}^1$ and $w^n=\mathsf{e}^{N+n+1}-\mathsf{e}^{N+1}$. The Laplacian matrix L acts on this basis as follows: $Lu^1=0$, $Lu^2=-2N\,u^2$ and $Lv^n=-N\,v^n$, $Lw^n=-N\,w^N$ for each $n=1,2,\ldots,N-1$. An initial condition $x\in\mathbb{R}^{2N}$ can be decomposed as

$$x=\bar{x}\,u^1+(\bar{x}_1-\bar{x})\,u^2+\sum_{n=1}^{N-1}\left((x_{n+1}-\bar{x}_1)\,v^n+(x_{N+n+1}-\bar{x}_2)\,w^n\right),$$

where

$$\bar{x}:=\frac{\sum_{n=1}^{2N}x_n}{2N},\ \bar{x}_1:=\frac{\sum_{n=1}^{N}x_n}{N}\ \text{ and }\ \bar{x}_2:=\frac{\sum_{n=1}^{N}x_{N+n}}{N}. \tag{19}$$

Therefore, for all $t \in \mathbb{R}$ we have

$$\begin{aligned} x(t) &= \bar{x}\, u^1 + e^{-2N\,t}(\bar{x}_1 - \bar{x})\, u^2 + e^{-Nt} \sum_{n=1}^{N-1} \left((x_{n+1} - \bar{x}_1), v^n + (x_{N+n+1} - \bar{x}_2)\, w^n\right), \\ &= \sum_{n=1}^{N} \left(\left(1 - e^{-Nt}\right)\left(\bar{x} - e^{-Nt}\bar{x}_1\right) + e^{-Nt}x_n\right) \mathsf{e}^n \\ &\qquad + \sum_{n=1}^{N} \left(\left(1 - e^{-Nt}\right)\left(\bar{x} - e^{-Nt}\bar{x}_2\right) + e^{-Nt}x_{N+n}\right) \mathsf{e}^{N+n}. \end{aligned}$$

From here it follows that

$$\begin{aligned} x_n(t) - x_{N+m}(t) &= e^{-N\,t}\left(x_n - x_{N+m} + \left(1 - e^{-Nt}\right)(\bar{x}_1 - \bar{x}_2)\right), \quad (20) \\ x_n(t) - x_m(t) &= e^{-N\,t}\,(x_n - x_m), \quad (21) \\ x_{N+n}(t) - x_{N+m}(t) &= e^{-N\,t}\,(x_{N+n} - x_{N+m}), \end{aligned}$$

for all $t \in \mathbb{R}$ and each $1 \leqslant m, n \leqslant N$. Hence, the distance between coordinates in the same party of $K_{N,N}$ decreases monotonously, while the distances between coordinates at different parties oscillate at most once, and then decrease to zero. All the differences decrease monotonously if and only if the initial condition satisfies $\bar{x}_1 = \bar{x}_2$. In this case the edges $\{n, m\}$ would be included in the synchronized subnetwork $G_{x(t)}$ for all $t \geqslant t_{n,m} := (\log|x_n - x_{N+m}| - \log(\epsilon))/N$.

Without lost of generality, we may assume that the initial condition is ordered as $x_1 \leqslant x_2 \leqslant \cdots \leqslant x_N$, $x_{N+1} \leqslant x_{N+2} \leqslant \cdots \leqslant x_{2N}$. By Equation (21) ensures that $x_1(t) \leqslant x_2(t) \leqslant \cdots \leqslant x_N(t)$ and $x_{N+1}(t) \leqslant x_{N+2}(t) \leqslant \cdots \leqslant x_{2N}(t)$ for all $t \in \mathbb{R}$. We will further assume, when convenient, that $\bar{x}_1 = \bar{x}_2$.

Once again, in order to take advantage of the fact that the Laplacian flow preserves the order of the coordinates at each party, we will define the transition diagram not over the synchronized subnetworks but over combinatorial objects that encode the synchronized subnetworks respecting this order. This will simplify the description the transition diagram, mainly in the monotonous case which is achieved when $\bar{x}_1 = \bar{x}_2$. We codify the ϵ-synchronized subnetwork G_x defined by $x_1 \leqslant x_2 \leqslant \cdots \leqslant x_N$, $x_{N+1} \leqslant x_{N+2} \leqslant \cdots \leqslant x_{2N}$, by the couple of

functions $\alpha_x, \omega_x : \{1, 2, \ldots, N\} \to \{0, 1, 2, \ldots, N+1\}$ given by

$$\alpha_x(n) = \begin{cases} \min\{\ell \leqslant N : x_n - \epsilon \leqslant x_{N+\ell}\} & \text{if } x_{2N} \geqslant x_n - \epsilon, \\ N+1 & \text{if } x_{2N} < x_n - \epsilon, \end{cases} \tag{22}$$

$$\omega_x(n) = \begin{cases} \max\{\ell \leqslant N : x_n + \epsilon \geqslant x_{N+\ell}\} & \text{if } x_{N+1} \leqslant x_n + \epsilon, \\ 0 & \text{if } x_{N+1} > x_n + \epsilon. \end{cases} \tag{23}$$

Notice that $\mathrm{im}(\alpha_x) \subset [1, N+1]$ while $\mathrm{im}(\omega_x) \subset [0, N]$. Both functions are increasing and such that $\alpha_x(n) \leqslant \omega_x(n) + 1$ for each $1 \leqslant n \leqslant N$. We present an example of the construction of the increasing functions from a given initial condition, in Figure 4.

Let $I_N := \{\phi : \{1, \ldots, N\} \to \{0, \ldots, N+1\} : \phi(n+1) \geqslant \phi(n) \text{ for all } 1 \leqslant n < N\}$. From the discussion in Appendix Appendix B, it follows that the collection

$$\Phi_{N,N} := \{(\alpha, \omega) : \alpha, \omega \in I_N : \mathrm{im}(\alpha) \subset [1, N+1], \mathrm{im}(\omega) \subset [0, N] \text{ and } \alpha \leqslant \omega + 1\}, \tag{24}$$

codifies all the ϵ-synchronized subnetworks of $K_{N,N}$ compatible with an ordered initial condition $x_1 \leqslant x_2 \leqslant \cdots \leqslant x_N$, $x_{N+1} \leqslant x_{N+2} \leqslant \cdots \leqslant x_{2N}$. The correspondence is given as follows. To $(\alpha, \omega) \in \Phi_{N,N}$ we associate the subnetwork $G_{(\alpha,\omega)} \subset K_{N,N}$ with edges in the set

$$E_{(\alpha,\omega)} = \{\{n, N+m\} : 1 \leqslant n, m \leqslant N, \text{ and } \alpha(n) \leqslant m \leqslant \omega(n)\}, \tag{25}$$

which is consistent with the fact that $(\alpha, \omega) = (\alpha_x, \omega_x)$ if and only if $G_{(\alpha,\omega)} = G_x$. The correspondence in Equation (25) establishes a mapping from $\Phi_{N,N}$ to the collection of ϵ-synchronized subnetworks defined by ordered initial conditions, in other words, it is in this case the λ mapping associated with Equation (5). The elements in $\Phi_{N,N}$ can be related to combinatorial objects, the parallelo-polyminoes inscribed in a given rectangle. The number of these objects is given by the so called the Narayana numbers [12]. A parallelo-polyminoe

in the rectangular lattice of size $p \times q$ is a connected union of squares delimited by two increasing boundary functions $L, U : \{1, 2, \ldots, p\} \to \{0, 1, \ldots, q\}$ such that $L(1) = 0$, $U(p) = q$, and $L(n) < U(n-1)$ for each $2 \leqslant n \leqslant p$.

The number of parallelo-polyminoes in the lattice of size $p \times q$ is given by the Narayana number [20]

$$T(p+q-1, q) := \frac{1}{p+q-1} \binom{p+q-1}{q} \binom{p+q-1}{q-1}. \tag{26}$$

To each couple $(\alpha, \omega) \in \Phi_{N,N}$ we associate a parallelo-polyminoe in $\{0, 1, \ldots, N+1\} \times \{0, 1, \ldots, N+1\}$ with border functions $L, U : \{1, \ldots, N+1\} \to \{0, 1, \ldots, N+1\}$, such that

$$L(n) = \begin{cases} 0 & \text{for } n = 1, \\ \alpha(n-1) - 1 & \text{for } 2 \leqslant n \leqslant N+1, \end{cases} \text{ and } U(n) = \begin{cases} \omega(n) + 1 & \text{for } 1 \leqslant n \leqslant N, \\ N+1 & \text{for } n = N+1. \end{cases} \tag{27}$$

In this way, we establish a one-to-one correspondence between parallelo-polyminoes and couples in $\Phi_{N,N}$, from which we obtain

$$|\Phi_{N,N}| = T(2N+1, N+1) = \frac{1}{2N+1} \binom{2N+1}{N+1} \binom{2N+1}{N}. \tag{28}$$

Thanks to the equivalence given by the Equation (9), each sequence of ϵ-synchronized subnetworks defined by an ordered initial condition is faithfully codified by the corresponding sequences of couples of increasing functions given by the Equations (22) and (23). As mentioned above, for an initial condition $x \in \mathbb{R}^{2N}$ such that $\bar{x}_1 = \bar{x}_2$, all the differences $x_{N+m}(t) - x_n(t)$ converge to 0 monotonously and at the same speed. We will say that such initial conditions are balanced. In this case, each one of the maps $t \mapsto \alpha_{x(t)}$ and $t \mapsto \omega_{x(t)}$ are coordinate-wise monotonous, and they converge respectively to the constant functions $\mathbf{1}(n) = 1$ and $\mathbf{N}(n) = N$ at time $t_{1,N} = (\log|x_1 - x_{2N}| - \log(\epsilon))/N$. The sequence of switching times $0 < t_1 < t_2 <$

$\cdots < t_\ell$ is such that $(\alpha_{x(t_\tau)}, \omega_{x(t_\tau)}) \neq (\alpha_{x(t_{\tau+1})}, \omega_{x(t_{\tau+1})})$. Let us denote α_{t_τ} by α_τ, and the corresponding for ω. For a typical initial condition, at each switching time only one of the functions α_τ or ω_τ changes and it changes only at one site. The sequence $((\alpha_0, \omega_0), (\alpha_1, \omega_1), \ldots, (\alpha_\ell, \omega_\ell))$ can be determined by the initial couple (α_0, ω_0), the jump sites $n_1, n_2, \ldots, n_\ell \in \{1, 2, \ldots, N\}^\ell$ and binary labels $q_1, q_2, \ldots, q_\ell \in (-1, +1)^\ell$ as follows:

$$(\alpha_{\tau+1}, \omega_{\tau+1}) = \begin{cases} (\alpha_\tau - \delta_{n_\tau}, \omega_\tau) & \text{if } q_\tau = -1, \\ (\alpha_\tau, \omega_\tau + \delta_{n_\tau}) & \text{if } q_\tau = +1. \end{cases} \tag{29}$$

To the couple $(\alpha_\tau, \omega_\tau)$, we can associate a parallelo-polyminoe according to Equation (27). In the transition $(\alpha_\tau, \omega_\tau) \to (\alpha_{\tau+1}, \omega_{\tau+1})$, the area inside the corresponding parallelo-polyminoe increases by one unit until the final area $N \times N$.

Realizable sequences $((n_1, q_1), (n_2, q_2), \ldots, (n_\ell, q_\ell))$, are those compatible with a balanced initial condition $x \in \mathbb{R}^{2N}$ and are completely determined by the differences $\Delta_{n,m} := x_{N+m} - x_n$ with $1 \leqslant n, m \leqslant N$ as follows: For $\epsilon < |\Delta_{n_1,m_1}| < |\Delta_{n_2,m_2}| < \cdots < |\Delta_{n_{N^2},m_{N^2}}|$ we have the sequence $((n_1, q_1), (n_2, q_2), \ldots, (n_{N^2}, q_{N^2}))$, where $q_\tau = \operatorname{sign}(\Delta_{n_\tau,m_\tau})$ for each $1 \leqslant \tau \leqslant N^2$. If we consider all the possible orderings $\Delta := \{\Delta_{n,m} : 1 \leqslant n, m \leqslant N\}$ compatible with an initial condition, not necessarily balanced, and we assume that the dynamics towards synchronization is completely determined by this ordering as in the balanced case, we obtain a transition diagram with vertices in $\Phi_{N,N}$ with maximal paths starting at the couples (α, ω) codifying the disconnected subnetwork, and ending at the couple $(\mathbf{1}, \mathbf{N})$ which codifies $K_{N,N}$. This digraph contains all the paths towards synchronization starting at balanced initial conditions but it also contains paths which are not compatible with any balanced initial condition. For instance, in the case $N = 2$ there are 20 realizable possible orderings $\{\Delta_{n,m} : 1 \leqslant n, m \leqslant N\}$, which we depict in Table 4, defining 20 paths towards synchronization represented in the transition diagram of Figure 6. Nevertheless, there are 4 orderings, and therefore 4 paths towards synchronization, which are incompatible with a balanced initial condition. The coordinate arrangements

incompatible with a balanced initial conditions are $x_1 < x_2 < x_3 < x_4$ and $x_3 < x_4 < x_1 < x_2$. In general there are 2 arrangements of initial conditions, $x_1 < \cdots < x_N < x_{N+1} < \cdots < x_{2N}$ and $x_{N+1} < \cdots < x_{2N} < x_1 < \cdots < x_N$, which are incompatible with a balanced initial condition. These arrangements define maximal paths starting at vertices $(\mathbf{1}, \mathbf{0})$ and $(\mathbf{N}+\mathbf{1}, \mathbf{N})$, which for the case $N = 2$ we indicate in red in Figure 6.

An easy upper bound for the number of paths towards synchronization starting at typical balanced initial conditions is the following. For each one of the arrangements $x_{i_1} < x_{i_2} < \cdots < x_{i_{2N}}$, obtained by inter-placing the first N coordinates with respect to the last N coordinates while maintaining the order inside each group of coordinates, there are Golomb$(2N)$ different orderings for the differences $x_{i_k} - x_{i_\ell}$. Each one of these orderings gives place to a path towards synchronization, but this path does not depend on the differences between coordinates of the same group (first N or last N coordinates). Furthermore, there are two coordinate arrangements which are incompatible with a balanced initial condition, when $x_1 < x_2 < \cdots < x_{2N}$ and when $x_{N+1} < x_{N+2} < \cdots < x_{2N} < x_1 < x_2 < \cdots < x_N$, hence the number of paths towards synchronization is upper bounded by

$$\text{Number of paths towards synchronization for } K_{N,N} \leqslant \left(\binom{2N}{N} - 2 \right) \text{Golomb}(2N). \tag{30}$$

As mentioned above, the growth of this quantity with respect to N defines a complexity function analogous to the topological complexity as a function of time.

Similar to the case K_N, the number of paths towards synchronization of a given length, $F_{N,N}(\ell)$, is given by the number of couples $(\alpha, \omega) \in \Phi_{N,N}$ such that the corresponding parallelo-polyminoe has an interior with area of $(N+1)^2 - \ell$

units. Hence,

$$F_{N,N}(\ell) := \left| \left\{ (\alpha, \omega) \in \Phi_{N,N} : \sum_{n=1}^{N+1} (U(n) - L(n)) = (N+1)^2 - \ell \right\} \right|. \quad (31)$$

Here, $L, U : \{1, \ldots, N+1\} \to \{0, 1, \ldots, N+1\}$ are the polyminoe border functions defined from the couple (α, ω) by Equations (27). Table 5 shows the distributions $F_{N,N}(\ell)$ for $2 \leqslant N \leqslant 8$.

For each N and $0 \leqslant \ell \leqslant N$, the integer $F_{N,N}(\ell)$ coincides with the ℓ-th term of the Sloans's sequence (Entry A000712 of the On-line Encyclopedia of Integer Sequences [21]), which among other things, counts the number of couples of integer partitions $P = (p_1 \geqslant p_2 \geqslant \cdots \geqslant p_k)$, $Q = (q_1 \geqslant q_2 \geqslant \cdots \geqslant q_r)$, such that $\sum_{i=1}^{k} p_i + \sum_{j=1}^{r} q_j = \ell$. Indeed, we can associate to each such couple of integer partitions (P, Q), a unique couple $L, U : \{1, 2, \ldots, N+1\} \to \{0, 1, \ldots, N+1\}$ of upper and lower border functions such that $U(i) = N+1-p_i$ and $L(N+2-j) = q_j$. Clearly $\sum_{i=1}^{k} p_i + \sum_{j=1}^{r} q_j = \ell$ if and only if the area of the parallelo-polyminoe with border functions L and U is $(N+1)^2 - \ell$. The correspondence between integer partitions and border functions cannot go further than $\ell = N$, since for $\ell = N+1$ the couple $((N+1), (0))$ of partitions does not define admissible border functions. On the opposite extreme, $F_{N,N}(N^2)$ counts all the parallelo-polyminoes in $\{0, 1, \ldots, N+1\} \times \{0, 1, \ldots, N+1\}$ composed of $2N+1$ squares. These squares are arranged in a path going from $(0, 0)$ to $(N+1, N+1)$, the next square place at the left or on top of the previous one. Each one of these arrangements can therefore by codified a sequences $(a_1, a_2, \ldots, a_{2N}) \in \{L, T\}^{2N}$, with exactly N entries equal to T. From this it follows that

$$F_{N,N}(N^2) = \binom{2N}{N} \quad (32)$$

The normalized cumulative distribution, $f_{N,N} : [0, 1] \to [0, 1]$, is given by

$$f_{N,N}(x) = \frac{1}{|\Phi_{N,N}|} \sum_{n \leqslant x \times N^2} F_{N,N}(x), \quad (33)$$

where $F_{N,N}$ is given by Equation (31) and $|\Phi_{N,N}|$ by Equation (28). We numerically computed $f_{N,N}(x)$ for increasing N, and observe how it approaches a limit distribution $x \mapsto \mathrm{f}(x)$ whose density $\varrho(x) := d\,\mathrm{f}(x)/dx$ approaches the curve depicted in Figure 7. As for K_N, our numerical computation suggest that ϱ is continuous, unimodal, and negatively skewed.

As we have already mentioned, in the case of $K_{N,N}$ we do not have the complete panorama of its paths towards synchronization, since our methodology is limited to the initial conditions that are balanced. In addition, currently there are no results in combinatorics that allow us to make calculations for arbitrarily large sizes. Nevertheless by directly computing these distributions for low dimensions, we observe a very fast convergence of the normalized distribution $f_{N,N}$. We obtain a unimodal distribution with maximum at

$$\mathrm{mode}_{N,N}(\ell) := \max_{1 \leqslant \ell \leqslant N^2} F_{N,N}(\ell) \approx 0.74118\, N^2. \tag{34}$$

as depicted in Figure 7. We observe that the distribution is negatively skewed, the mean length of these paths being larger than the most frequent length,

$$\langle \ell \rangle_{N,N} := \frac{\sum_{\ell=1}^{N^2} \ell\, F_{N,N}(\ell)}{T(2N+1, N+1)} \approx 0.8125\, N^2 > \mathrm{mode}_{N,N}(\ell).$$

The above estimations were obtained by using a relatively low (N=8) dimension. As mentioned above, already at this low dimension we obtain the accurate qualitative behavior of the asymptotic distribution. In this way we can qualitatively describe a typical synchronization path for the Laplacian of the complete bipartite graph, starting at a random balanced ordered initial condition of dimension $2N$. For instance, such a synchronization path would most likely be of the length indicated in Equation (34).

6. Remark and comments

Thanks to the monotonic behavior of the Laplacian flow in K_N, it was possible to completely describe the behavior of the transient dynamics of the system via a codification of the synchronized subnetworks by increasing functions. In the case of $K_{N,N}$, the monotonic behavior holds separately, for the coordinates at each one of the parties of $K_{N,N}$, which allows a codification by couples of increasing functions. A global monotonic behavior is verified only by paths towards synchronization starting at balanced initial conditions. Those are precisely the paths that follow the computed transition diagram. It is important to note that this kind of monotonic convergence towards synchronization is only possible in graphs with large spectral degeneracy as it is the case for K_N and $K_{N,N}$. This monotonicity does not hold, for instance, for cycle graphs or ring lattices for which another kind of coding and transition diagram is needed.

For both, the Laplacian flow in K_N and $K_{N,N}$, we obtained closed formulae for the number of realizable synchronized subnetworks, which are codified by known combinatorial objects. Although we do not dispose of closed formulae for the number of paths towards synchronization, which can be seen as a complexity function, we can nevertheless easily obtain factorial upper and lower bounds.

The probability density functions of asymptotic normalized lengths of paths towards synchronization, in both cases, are continuous, unimodal, and negatively skewed. The typical length relative to the longest path is larger for $K_{N,N}$ than for K_N.

In Section 4 we studied the applicability of the Kuramoto model, of the combinatorial description proper to the Laplacian flow in K_N. Although the codification of synchronized subnetworks by increasing functions is pertinent in the nonlinear case, the transition diagram applies only to initial conditions in a neighborhood of the synchronization manifold, and only after a finite transient that depends on the initial condition.

Regarding the applicability of the combinatorial description of the Laplacian flow in $K_{N,N}$ to the corresponding Kuramoto model, we can already verify that the nonlinear dynamics preserves as well the cyclic order of the coordinates at

each of the two parties. For this, we proceed as in Section 4 and obtain

$$\begin{aligned}\frac{d(x_n - x_m)}{dt} &= -2R_2\sigma \sin\left(\frac{x_{N+n} - x_{N+m}}{2}\right)\cos\left(\Theta_1 - \frac{x_{N+n} + x_{M+m}}{2}\right),\\ \frac{d(x_{N+n} - x_{N+m})}{dt} &= -2R_1\sigma \sin\left(\frac{x_n - x_m}{2}\right)\cos\left(\Theta_1 - \frac{x_n + x_m}{2}\right),\end{aligned}$$

with $R_1\, e^{i\Theta_1} = \left(\sum_{k=1}^{N}\cos(x_k)\right) + i\left(\sum_{k=1}^{N}\sin(x_k)\right)$ and similarity for $R_2\, e^{i\Theta_2}$. Following the same argument as in Section 4, we deduce that two coordinates cannot merge in finite time and therefore the cyclic order of the coordinates at each party is preserved by the Kuramoto flow. This allows us to use the coding of ϵ-synchronized subnetworks defined for the Laplacian flow in Section 5.

As already mentioned, the transition diagram defined for the Laplacian flow over $K_{N,N}$ describes only the paths toward synchronization corresponding to balanced initial conditions. In Figure 6, we marked in red the subnetworks incompatible with balanced initial conditions. A complete transition diagram, which would contain those subnetworks, would include non-monotonous paths. Furthermore, for unbalanced initial conditions, the order in the differences between coordinates is not preserved by the flow. The description of the full transition diagram for the Laplacian flow over $K_{N,N}$ as well as the applicability of this description to the nonlinear case, would be the subject of future work. When considering Kuramoto models on large dimensions or on cyclic networks, another kind of synchronized regime imposes where vortex-like solutions attract a large volume of initial conditions. An extension of our approach is necessary to describe this kind of synchronization.

Finally we would like to emphasize that these synchronizing sequences can be seen as partitioning the basin of attraction of a given attractor (here the fully synchronized state). Since for a given finite ϵ the final synchronized network will be reached in a finite time $\tau(\epsilon, N)$, if the space of initial conditions has a finite volume, the full space-time will be as well bounded, and these sequences are partitioning that full space time. Moreover, by associating to a given sequence an ensemble of initial conditions realizing that sequence, we should be able

to measure that ensemble and add corresponding weights (measures) to each sequence and characterize even further the space-time complexity.

Acknowledgements

The authors are grateful for the financial support from ECOS-CONACyT-ANUIES through Grant M16M01. A. E. benefits from the National Scholarship No. 722957 offered by CONACyT-México. She thanks Fundación Sofia Kovalevskaia and Sociedad Matemática Mexicana for financial support. E. U. benefited from a research stay at the Centre de Physique Théorique-Luminy, financed by the CNRS-France.

References

[1] A. Pikovsky, M. Rosenblum, J. Kurths, Synchronization - a universal concept in nonlinear sciences, in: Cambridge Nonlinear Science Series, 2001.

[2] Y. Kuramoto, Self-entrainment of a population of coupled non-linear oscillators, in: H. Araki (Ed.), International Symposium on Mathematical Problems in Theoretical Physics, Springer Berlin Heidelberg, Berlin, Heidelberg, 1975, pp. 420–422.

[3] S. H. Strogatz, From kuramoto to crawford: exploring the onset of synchronization in populations of coupled oscillators, Physica D: Nonlinear Phenomena 143 (2000) 1–20.

[4] A. Arenas, A. Diaz-Guilera, J. Kurths, Y. Moreno, C. Zhou, Synchronization in complex networks, Physics Reports 469 (2008) 93–153.

[5] W. Ren, R. W. Beard, E. M. Atkins, A survey of consensus problems in multi-agent coordination, Proceedings of the 2005, American Control Conference, 2005. (2005) 1859–1864 vol. 3.

[6] A. P. Millán, J. J. Torres, G. Bianconi, Synchronization in network geometries with finite spectral dimension, Phys. Rev. E 99 (2019) 022307.

[7] V. Afraimovich, G. M. Zaslavsky, Space-time complexity in hamiltonian dynamics, Chaos 13 (2003) 519–532.

[8] G. M. Zaslavsky, V. Afraimovich, Working with complexity functions, in: P. Collet, M. Courbage, S. Métens, A. Neishtadt, G. Zaslavsky (Eds.), Chaotic Dynamics and Transport in Classical and Quantum Systems, Springer Netherlands, Dordrecht, 2005, pp. 73–85.

[9] X. Leoncini, G. M. Zaslavsky, Jets, stickiness and anomalous transport, Physical Review E : Statistical, Nonlinear, and Soft Matter Physics 65 (2002) 046216. 17 pages, 17 figures.

[10] A. Arenas, A. Díaz-Guilera, C. J. Pérez-Vicente, Synchronization reveals topological scales in complex networks, Phys. Rev. Lett. 96 (2006) 114102.

[11] A. Barrat, B. Fernandez, K. K. Lin, L.-S. Young, Modeling temporal networks using random itineraries, Phys. Rev. Lett. 110 (2013) 158702.

[12] R. P. Stanley, S. Fomin, Enumerative Combinatorics, volume 2 of *Cambridge Studies in Advanced Mathematics*, Cambridge University Press, 1999. doi:10.1017/CBO9780511609589.

[13] S. W. Golomb, How to number a graph, in: R. C. READ (Ed.), Graph Theory and Computing, Academic Press, 1972, pp. 23–37. URL: https://www.sciencedirect.com/science/article/pii/B9781483231877500088. doi:https://doi.org/10.1016/B978-1-4832-3187-7.50008-8.

[14] R. Hildebrand, Positive partial transpose from spectra, Physical Review A 76 (2007) 052325:1–052325:5.

[15] N. Johnston, A237749, https://oeis.org/A237749, 2014. [Online; accessed 04-May-2022].

[16] R. M. Thrall, A combinatorial problem., Michigan Mathematical Journal 1 (1952) 81 – 88.

[17] N. Johnston, Counting the Possible Orderings of Pairwise Multiplication, http://www.njohnston.ca/2014/02/counting-the-possible-orderings-of-pairwise-multiplication/, 2014. [Online; accessed 04-May-2022].

[18] L. Carlitz, J. Riordan, Two element lattice permutation numbers and their q-generalization, Duke Mathematical Journal 31 (1964) 371–388.

[19] S. A. Blanco, T. K. Petersen, Counting dyck paths by area and rank, Annals of Combinatorics 18 (2012) 171–197.

[20] E. Barcucci, A. Frosini, S. Rinaldi, On directed-convex polyominoes in a rectangle, Discrete Mathematics 298 (2005) 62–78. Formal Power Series and Algebraic Combinatorics 2002 (FPSAC'02).

[21] N. J. A. Sloane, A000712, https://oeis.org/A000712, 2022. [Online; accessed 04-May-2022].

Appendix A.

For each increasing function $\phi : \{1, 2, \dots, N\} \to \{1, 2, \dots, N\}$ such that $\phi \geqslant \mathrm{Id}$, there exists an ordered initial condition $x \in \mathbb{R}^N$ such that $\phi = \phi_x$. For this we use a representation of ϕ as a disjoint union of directed trees as follows. Let $\mathrm{Fix}(\phi) := \{1 \leqslant n \leqslant N : \phi(n) = n\}$. To each $n \in \mathrm{Fix}(\phi)$ we associate a directed tree T_n, rooted at n, with vertex set $V_n := \bigcup_{l=0}^{h(n)} \phi^{-l}(\{n\})$ and directed edges in $A_n := \{(k, \phi(k)) : k \in V_n \backslash \{n\}\}$. The vertex set V_n splits into $h(n) + 1$ disjoint levels, $V_n^l := \phi^{-l}(\{n\})$, $0 \leqslant l \leqslant h(n)$. The number $h(n)$ is the high T_n. The maximal paths in T_n are completely determined by their starting vertices, which have to be leaves. Let $\ell_n^1 < \ell_n^2 < \cdots < \ell_n^{w(n)}$ be the leaves of T_n. Its number, $w(n)$, is the width of the tree T_n. Since ϕ is increasing and such that $\phi \geqslant \mathrm{Id}$, then every element in the l-th level, V_n^l, is greater than all the elements in the l'-th level, $V_n^{l'}$ whenever $l < l'$. It implies that the length $l(m)$ of the path starting at m and ending at the root, is a decreasing function of m. Each

maximal path in T_n starts at a leaf and the longest of those paths have length $h(n)$, and start at leaves in the highest level. Furthermore, all vertices in T_n belong to a maximal path, which means that it is reachable from a leaf.

Now, given $\phi : \{1, 2, \dots, N\} \to \{1, 2, \dots, N\}$ increasing and such that $\phi \geqslant \mathrm{Id}$, let $\{T_{n_k} : 1 \leqslant k \leqslant R\}$ be the associated collection of directed trees and $n_1 < n_2 < \cdots < n_R$ in $\mathrm{Fix}(\phi)$ the corresponding roots. Define $x \in \mathbb{R}^N$ such that $x_{n_1} = \epsilon\, h(n_1)$, and for each $1 \leqslant k < R$,

$$x_{n_{k+1}} = x_{n_k} + (h(n_k) + 2)\,\epsilon. \tag{A.1}$$

In this way, we fix the value of x_n for each $n \in \mathrm{Fix}(\phi)$ in such a way that $x_{n_k} + \epsilon < x_{n_{k+1}} - h(n_{k+1})\,\epsilon$ for each $1 \leqslant k < R$. Now, for each $n \in \mathrm{Fix}(\phi)$, let $\ell_n^1 < \ell_n^2 < \cdots < \ell_n^{w(n)}$ be the leaves of T_n. For each $1 \leqslant j \leqslant w(n)$ and $0 \leqslant k \leqslant l(n_j)$ for which $x_{\phi^k(\ell_n^j)}$ is not yet defined, let

$$x_{\phi^k(\ell_n^j)} = x_n - (l(n_j) - k)\,\epsilon + (j-1)\frac{\epsilon}{w(n)}. \tag{A.2}$$

Let us remind that $l(n_j)$ is the length of the maximal path starting at ℓ_n^j. It is not difficult to verify that Equations (A.1) and (A.2) define an ordered initial condition $0 = x_1 < x_2 < \cdots < x_N = \sum_{k=1}^{R}(h(n_k) + 2)$, such that $\phi_x = \phi$.

Appendix B.

Each couple of increasing functions $\alpha, \omega : \{1, \dots, N\} \to \{0, 1, \dots, N+1\}$ is compatible with some $x \in \mathbb{R}^{2N}$ in terms of the Equations (22) and (23), and therefore codify an ϵ-synchronized subnetwork, provided $\mathrm{im}(\alpha) \subset [1, N+1]$, $\mathrm{im}(\omega) \subset [0, N]$ and $\alpha \leqslant \omega + 1$. Such an initial condition can be constructed as follows.

For each $1 \leqslant n \leqslant N$ let $\mathcal{A}_n := \{1 \leqslant m \leqslant N : \alpha(n) \leqslant m \leqslant \omega(n)\}$. Let us partition $\{1, 2, \dots, N\} = \bigsqcup_{k=1}^{\ell} I_k$, where for each $1 \leqslant k \leqslant \ell$, $I_k = \{n_k, n_k + 1, \dots, m_k\}$ is such that $\mathcal{A}_n \cap \mathcal{A}_{n+1} \neq \varnothing$ for each $n_k \leqslant n < m_k$ and it is a maximal element in the sense of inclusion ($I_k \subsetneq I \Rightarrow \bigcup_{n \in I_k} \mathcal{A}_n$ is not an interval). Notice that $n_1 = 1$ and that $I_k = \{n_k\}$ whenever $\alpha(n_k) = \omega(n_k) + 1$.

For each $1 < k \leqslant \ell$, let $\Delta : I_k \to I_k$ be such that $\Delta(n) = \max\{m \in I_k : \mathcal{A}_n \cap \mathcal{A}_m \neq \varnothing\}$. Clearly $\Delta(n) \geqslant n$ and $\Delta(n) = n$ if and only if $n = n_k = m_k$. We can associate to Δ a directed tree T_k with vertices in I_k, rooted at m_k, and arrows $n \mapsto \Delta(n)$. The structure of these trees is similar to that of the trees described in Appendix Appendix B. Let $n_k \mapsto \Delta(n_k) \mapsto \cdots \mapsto \Delta^j(n_k) \mapsto \cdots \mapsto m_k = \Delta^{h_k}(n_k)$ be the maximal path in T_k and for each $1 \leqslant j \leqslant l_k$ let $V_j = \Delta^{-j}(\{m_k\})$ be the j-th level of T_k. Clearly $\min V_j = \Delta^{h_k - j}(n_k)$ and $\max V_j < \min V_{j-1}$ for each $0 \leqslant j \leqslant h_k$.

Assume x_{n_k} is given. Let $n_{k,j} := \min V_j$ and define $x_{n_{k,j}} := x_{n_k} + j\epsilon$ for each $1 \leqslant j \leqslant h_k$. Now, for $n_{k,j} \leqslant n < n_{k,j-1}$, let $x_n = x_{n_{k,j}} + (n - n_{k,j})\,\epsilon/(n_{j-1} - n_{k,j})$. With $\delta_k := \frac{1}{2}\min_{n_k \leqslant n < m_k}(x_{n+1} - x_n)$, for each $n_k \leqslant n < m_k$ and $\alpha(n) \leqslant m < \alpha(n+1)$, let $x_{N+m} = x_n - (\epsilon - \delta_k)$. For $n_{k,1} \leqslant n < n_{k,0} \equiv m_k$ and $\omega(n) < m \leqslant \omega(n+1)$, let $x_{N+m} = x_n + (\epsilon - \delta_k)$. Finally, for $\alpha(m_k) \leqslant m \leqslant \omega(n_{k,1})$, define $x_{N+m} = (x_{n_{k,1}} + x_{m_k})/2$.

In order to complete the specification of all the coordinate, fix $x_1 = x_{n_1} = 0$ and for each $1 \leqslant k \leqslant \ell$ let $x_{n_k} := x_{m_{k-1}} + 3\epsilon$. Finally, for each $m \notin \bigcup_{n=1}^{N} \mathcal{A}_n$, let $k(m) := \min\{1 \leqslant k \leqslant \ell : \alpha(n_k) > m\}$ and define $x_{N+m} := x_{N+\alpha(n_k)} - 3\epsilon/2$. If $\omega(N) < N$, then define $x_{N+m} := x_{m_\ell} + 3\epsilon/3$.

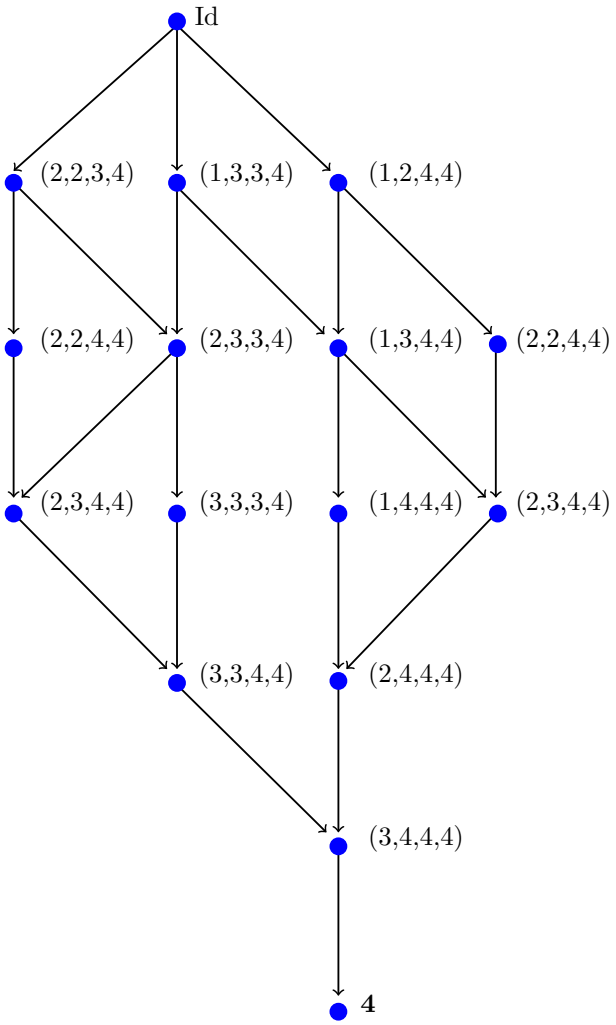

Figure 2: The transition diagram which contains all the paths towards synchronization of the Laplacian dynamics on K_4. The synchronized subgraphs are encoded by increasing functions as defined by Equation (9). At the top is placed the identity function Id := $(1, 2, 3, 4)$ which codifies the completely disconnected graph. All the paths end at the constant function $\mathbf{4} = (4, 4, 4, 4)$, which codifies the globally synchronized state

.

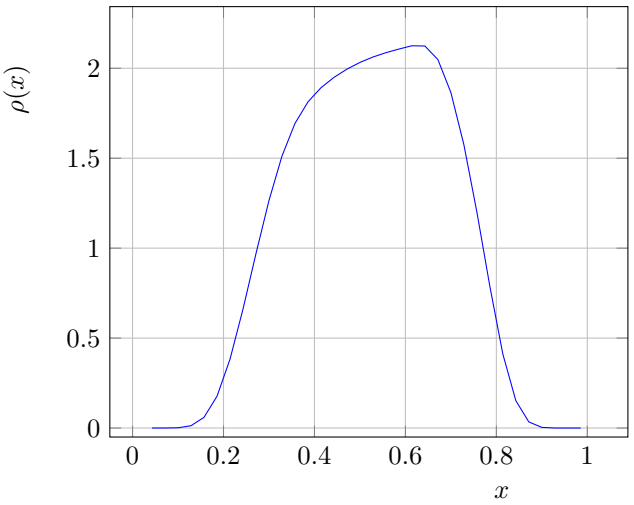

Figure 3: The probability density function $\rho(x)$ of the asymptotic distribution of the normalized length of a path towards synchronization. For N sufficiently large and $\delta > 0$ sufficiently small, the proportion of paths of length $N(N-1)(x \pm \delta)/2$ is approximatively $\rho(x)\,\delta$.

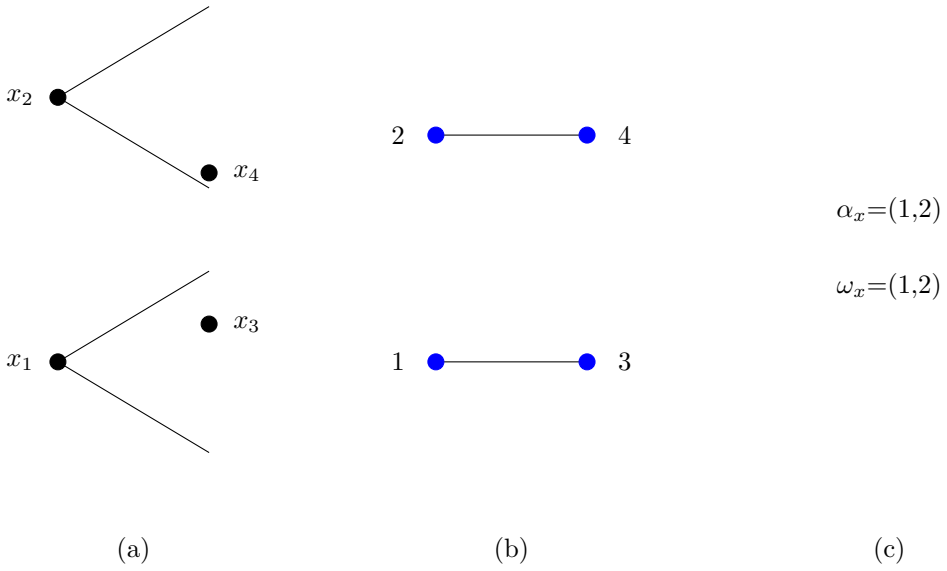

Figure 4: In (a), an example of the relative position of the coordinates of $x = (x_1, x_2, x_3, x_4)$ is illustrated with black dots. The angles that opens from the first two coordinates indicate their ϵ-neighborhood. To construct G_x, according to Equation (25), it is enough to observe that x_3 is inside the ϵ-neighborhood of x_1, and also x_4 is inside the ϵ-neighborhood of x_2, hence in (b), vertices 1 and 3 are connected as well as vertices 2 and 4. In (c), the increasing functions determined by x are shown. The function α_x codified the fact that x_3 is the first coordinate of the second party inside the angle opening from x_2 and similarly x_4 with respect to x_2. On the other hand, ω_x, indicates that x_3 is the last coordinate of the second party inside the angle opening from x_1 and respectively x_4 with respect to x_2.

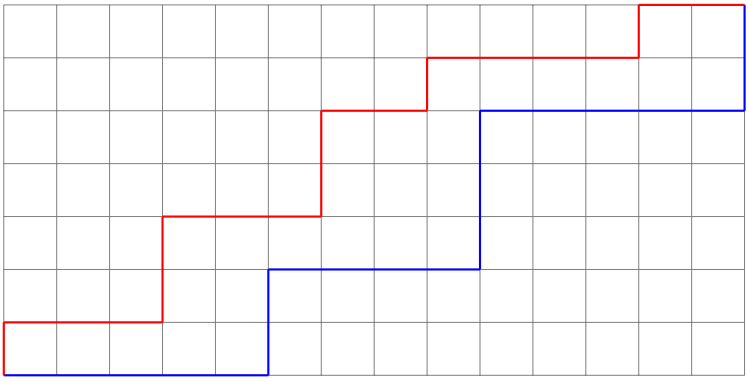

Figure 5: A parallelo-polyminoe in the lattice of size 14×10. The blue path defines the lower border function $L = (0, 0, 0, 0, 0, 2, 2, 2, 5, 5, 5, 5, 5)$, while the red one defines the upper border $U = (1, 1, 1, 3, 3, 3, 5, 5, 6, 6, 6, 6, 7, 7)$.

Coordinates	Differences	Signs
$x_1 < x_2 < x_3 < x_4$	$\lvert\Delta_{2,1}\rvert < \lvert\Delta_{2,2}\rvert < \lvert\Delta_{1,1}\rvert < \lvert\Delta_{1,2}\rvert$	$(+1,+1,+1,+1)$
	$\lvert\Delta_{2,1}\rvert < \lvert\Delta_{1,1}\rvert < \lvert\Delta_{2,2}\rvert < \lvert\Delta_{1,2}\rvert$	$(+1,+1,+1,+1)$
$x_1 < x_3 < x_2 < x_4$	$\lvert\Delta_{2,1}\rvert < \lvert\Delta_{2,2}\rvert < \lvert\Delta_{1,1}\rvert < \lvert\Delta_{1,2}\rvert$	$(-1,+1,+1,+1)$
	$\lvert\Delta_{2,2}\rvert < \lvert\Delta_{2,1}\rvert < \lvert\Delta_{1,1}\rvert < \lvert\Delta_{1,2}\rvert$	$(+1,-1,+1,+1)$
	$\lvert\Delta_{2,2}\rvert < \lvert\Delta_{1,1}\rvert < \lvert\Delta_{2,1}\rvert < \lvert\Delta_{1,2}\rvert$	$(+1,+1,-1,+1)$
	$\lvert\Delta_{2,1}\rvert < \lvert\Delta_{1,1}\rvert < \lvert\Delta_{2,2}\rvert < \lvert\Delta_{1,2}\rvert$	$(-1,+1,+1,+1)$
	$\lvert\Delta_{1,1}\rvert < \lvert\Delta_{2,1}\rvert < \lvert\Delta_{2,2}\rvert < \lvert\Delta_{1,2}\rvert$	$(+1,-1,+1,+1)$
	$\lvert\Delta_{1,1}\rvert < \lvert\Delta_{2,2}\rvert < \lvert\Delta_{2,1}\rvert < \lvert\Delta_{1,2}\rvert$	$(+1,+1,-1,+1)$
$x_1 < x_3 < x_4 < x_2$	$\lvert\Delta_{1,1}\rvert < \lvert\Delta_{2,2}\rvert < \lvert\Delta_{1,2}\rvert < \lvert\Delta_{2,1}\rvert$	$(+1,-1,+1,-1)$
	$\lvert\Delta_{2,2}\rvert < \lvert\Delta_{1,1}\rvert < \lvert\Delta_{2,1}\rvert < \lvert\Delta_{1,2}\rvert$	$(-1,+1,-1,+1)$
$x_3 < x_4 < x_1 < x_2$	$\lvert\Delta_{1,2}\rvert < \lvert\Delta_{1,1}\rvert < \lvert\Delta_{2,2}\rvert < \lvert\Delta_{2,1}\rvert$	$(-1,-1,-1,-1)$
	$\lvert\Delta_{1,2}\rvert < \lvert\Delta_{2,2}\rvert < \lvert\Delta_{1,1}\rvert < \lvert\Delta_{2,1}\rvert$	$(-1,-1,-1,-1)$
$x_3 < x_1 < x_4 < x_2$	$\lvert\Delta_{1,2}\rvert < \lvert\Delta_{1,1}\rvert < \lvert\Delta_{2,2}\rvert < \lvert\Delta_{2,1}\rvert$	$(+1,-1,-1,-1)$
	$\lvert\Delta_{1,1}\rvert < \lvert\Delta_{1,2}\rvert < \lvert\Delta_{2,2}\rvert < \lvert\Delta_{2,1}\rvert$	$(-1,+1,-1,-1)$
	$\lvert\Delta_{1,1}\rvert < \lvert\Delta_{2,2}\rvert < \lvert\Delta_{1,2}\rvert < \lvert\Delta_{2,1}\rvert$	$(-1,-1,+1,-1)$
	$\lvert\Delta_{1,2}\rvert < \lvert\Delta_{2,2}\rvert < \lvert\Delta_{1,1}\rvert < \lvert\Delta_{2,1}\rvert$	$(+1,-1,-1,-1)$
	$\lvert\Delta_{2,2}\rvert < \lvert\Delta_{1,2}\rvert < \lvert\Delta_{1,1}\rvert < \lvert\Delta_{2,1}\rvert$	$(-1,+1,-1,-1)$
	$\lvert\Delta_{2,2}\rvert < \lvert\Delta_{1,1}\rvert < \lvert\Delta_{1,2}\rvert < \lvert\Delta_{2,1}\rvert$	$(-1,-1,+1,-1)$
$x_3 < x_1 < x_2 < x_4$	$\lvert\Delta_{1,1}\rvert < \lvert\Delta_{2,2}\rvert < \lvert\Delta_{1,2}\rvert < \lvert\Delta_{2,1}\rvert$	$(-1,+1,+1,+1)$
	$\lvert\Delta_{2,2}\rvert < \lvert\Delta_{1,1}\rvert < \lvert\Delta_{2,1}\rvert < \lvert\Delta_{1,2}\rvert$	$(+1,-1,-1,+1)$

Table 4: The twenty different orderings of the differences between coordinates at opposite parties, and corresponding signs, for a typical initial conditions in $\mathbb{R}^4$.

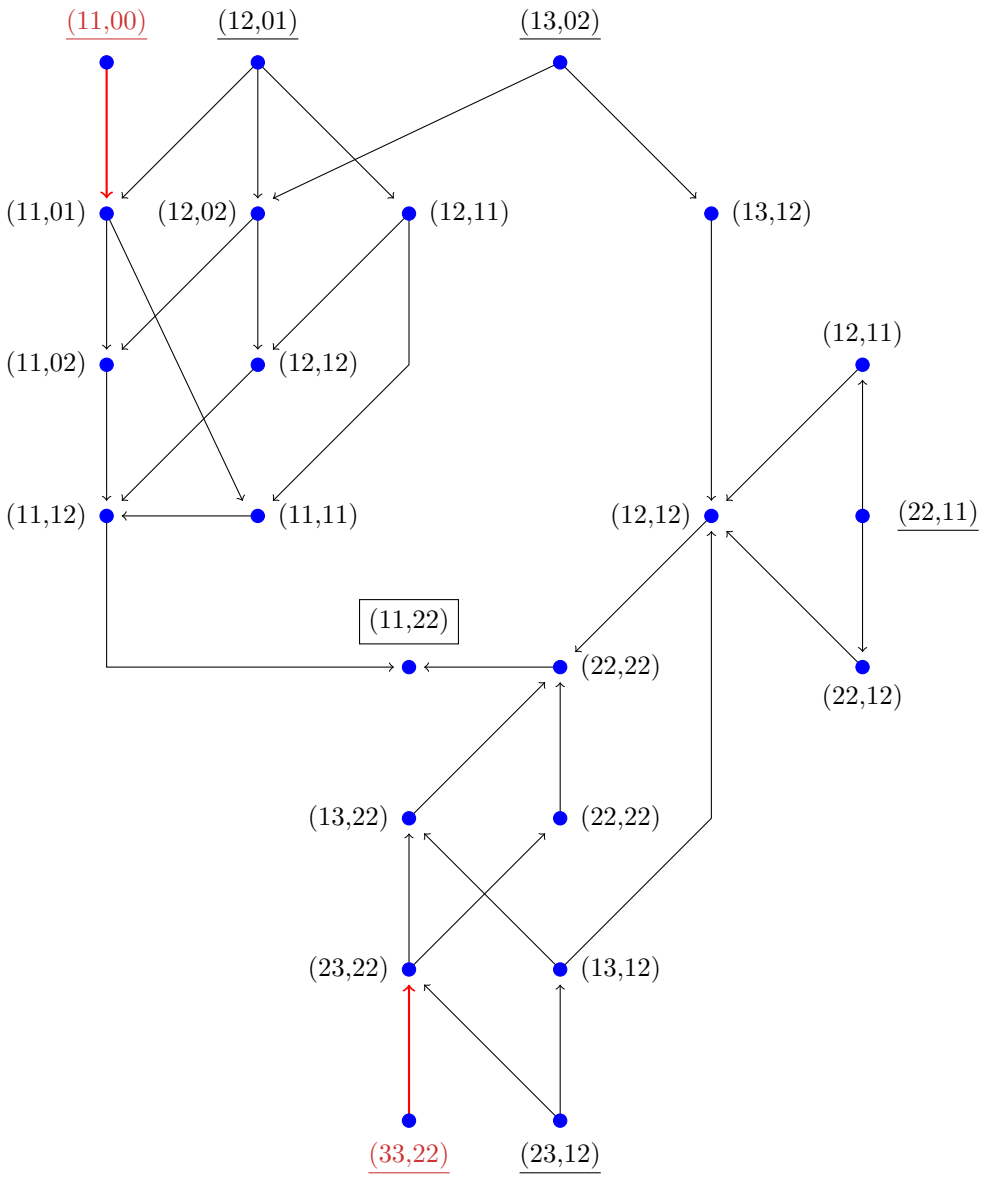

Figure 6: The transition diagram which contains all the paths towards synchronization of the Laplacian dynamics on $K_{2,2}$. Each one of the functions α, ω, are codified by a two-digit string. There are six starting configurations, underlined in the diagram, all of them coding the disconnected network. The ending vertex, $(11, 22)$, is the couple codifying the complete bipartite graph $K_{2,2}$. In red we indicate the starting couples which are incompatible with a balanced initial condition. In this case, by erasing the elements in color red, we obtain the transition diagram codifying all the paths towards synchronization for balanced initial conditions.

N	$F_{N,N}(\ell)$
2	(1,2,5,6,6)
3	(1,2,5,10,16,24,31,36,30,20)
4	(1,2,5,10,20,32,53,78,111,146,187,216,243,240,210,140,70)
5	(1,2,5,10,20,36,61,98,153,228,327,454,611,798,1005,1236,1466,1688,1862,1980,1971, 1850,1540,1120,630,252)
6	(1,2,5,10,20,36,65,106,173,268,409,600,867,1212,1671,2244,2966,3826,4868,6056, 7422,8906,10519,12166,13830,15352,16704,17656,18133,17890,16903,14966,12306, 8988,5670,2772,924)
7	(1,2,5,10,20,36,65,110,181,288,449,680,1013,1474,2107,2958,4088,5558,7450,9842, 12820,16488,20932,26246,32507,39790,48116,57538,67984,79414,91653,104578,117806, 131096,143865,155692,165779,173530,177877,178282,173616,163632,147855,127092, 102060,75432,49434,27720,12012,3432)
8	(1,2,5,10,20,36,65,110,185,296,469,720,1093,1618,2369,3400,4824,6732,9296,12654, 17054,22694,29912,38976,50333,64320,81489,102242,127219, 156850,191841,232602, 279832,333830,395204,464030,540737,625028,716966,815766,920990,1031168,1145253, 1260882,1376172,1487820,1593022,1687242,1766791,1826112,1860845,1865122, 1834995,1765746,1656541,1506540,1320987,1106748,877470,647592,437118,260832, 132132,51480,12870)

Table 5: Number $F_{N,N}(\ell)$ of couples $(\alpha, \omega) \in \Phi_{N,N}$ codifying a subnetworks starting a synchronizing path of length ℓ.

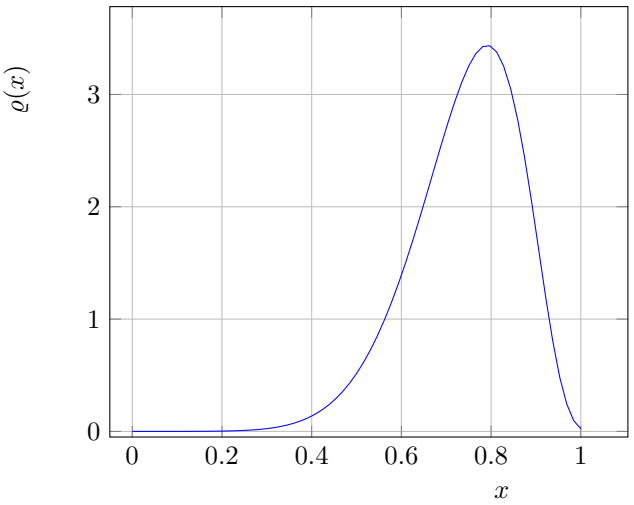

Figure 7: The probability density function $\varrho(x)$ of the asymptotic distribution of the normalized length of a path towards synchronization. For N sufficiently large and $\delta > 0$ sufficiently small, the number of paths of length $N^2(x \pm \delta)/2$ is approximatively $\varrho(x)\,\delta$.